

## SSC ANALYSIS OF THE GEMS FOR REACTIVITY CONTROL IN PRISM\*

G.C. Slovik and J. Rodnizki  
Brookhaven National Laboratory

BNL-NUREG--47978

DE93 007280

**Abstract**

The performance of three Gas Expansion Modules (GEMs) utilized in the Advanced Liquid Metal Reactor (ALMR) concept, PRISM, was analyzed using the computer code, SSC. GE has submitted the PRISM design for a Pre-application Safety Evaluation Report (PSER). The draft PSER indicated a potential weakness in the Unscrammed Loss of Flow (ULOF) event, and GE modified the design by adding three GEMs. These devices act like manometers and insert negative reactivity feedback into the core, relative to nominal operating conditions, when the pressure (or core flow) is reduced at the core inlet.

The PRISM design was analyzed by SSC for two cases. First, the design's original response to a ULOF where one Electro Magnetic (EM) pump fails to produce a coastdown was analyzed. Then the revised design with the GEMs included was analyzed. The original design had little or no safety margin for this case. The peak fuel temperature in the hot channel was predicted to be 1358K, which is above the solidus temperature of the fuel. However, after the GEMs were added, the loss of one EM pump coastdown became a benign event. The GEM feedback was predicted by SSC to dominate the other reactivity feedbacks and the GEMs, essentially, responded like passive control rods. The fuel temperature quickly dropped below operating temperatures, while the margin to sodium boiling was predicted to be greater than 350K.

**1.0 INTRODUCTION**

PRISM, an Advanced Liquid Metal Reactor (ALMR) with metal fuel, is presently under pre-application licensing review by the NRC, with Brookhaven National Laboratory (BNL) providing technical assistance. In this paper, we'll describe the impact the Gas Expansion Modules (GEMs) have on the predicted performance of PRISM during Unprotected (i.e. no scram) Loss of Flow (ULOF) events.

The initial PRISM design, as submitted for the preapplication review, relied on the "passive shutdown mechanism" to reduce the power during postulated heat up events. The "passive shutdown mechanism" relies largely on the increase in volume, and therefore neutron leakage, from thermal expansion of structural components in the core, such as: fuel axial expansion, core radial expansion (from the above core load pads and the grid plate), and control rod drive line expansion. This passive shutdown mechanism works well, except in a few improbable cases where the power-to-flow ratio increases very quickly. In these cases, the long time constants (i.e. long relative to the time frame they are needed) of the thermal feedbacks prevent a fast response to overcome the positive feedbacks from the sodium density (and potentially a positive void feedback).

For the Draft Pre-application Evaluation Safety Report (DPSER) for PRISM

\*This work was performed under the auspices of the U.S. Nuclear Regulatory Commission

**MASTER**

DISTRIBUTION OF THIS DOCUMENT IS UNLIMITED

YR

(Ref. 1) the system was evaluated, and a potential weakness in ULOFs with EM pump failures was noted. Since the release of that document, the applicant, General Electric (GE), has revised the PRISM design for consideration before the Final Pre-application Safety Evaluation Report is issued. In several cases, the changes were made to directly address the NRC concerns in the DPESR. Other changes were dictated by the U.S. Department of Energy (DOE) as design improvements or revisions to enhance the economics of the plant. However, the addition of three GEMs on the core periphery was arguably the most significant change from a safety perspective.

Gas Expansion Modules (GEMs) are designed to provide additional negative reactivity feedback during loss of primary flow events. The device is essentially an empty assembly duct, sealed at the top, open at the bottom, and connected to the core high pressure inlet plenum. Inside is a volume of cover gas that is trapped during the loading process. The objective is to control radial neutron leakage from the core. When the pumps are at full flow, the high inlet plenum pressure compresses the gas in the GEM cavity to a level above the core, providing neutron backscatter into the fuel from the sodium. When the flow decreases, the trapped gas expands, displacing the sodium in the fuel region with gas. The gas scatters fewer neutrons back into the core, causing a negative reactivity feedback. The reactivity worth of the GEMs is predicted to be 69 cents when the gas bubble transverses the full length of the fuel (i.e. a gas stroke that travels from the top of the core to the bottom).

The GEM model addition to the SSC model, and subsequent calculations resulted in very different behavior during postulated ULOF events, when compared to the previous design. The initial design had only the passive shutdown mechanisms to preserve an acceptable power-to-flow ratio. Under some cases this resulted in a fast increase in the power-to-flow ratio. The net result was that the margin to sodium boiling was predicted to be only a few degrees for some highly improbable events. In particular, ULOF events that were postulated to proceed missing one or more EM pump coastdowns, as provided by the "synchronous machines" (motor-generator sets running in parallel), had little or no safety margin. Fuel temperatures in the hot and average channel were calculated to be 1358K, (which is above the solidus temperature of metal fuel) and 1147K (Ref. 2). However, after the GEMs were added, the loss of one EM pump coastdown became a benign event. The GEM worth dominated the other reactivity feedbacks and the GEMs, essentially, responded like passive control rods. The fuel temperatures quickly dropped below operating conditions, while the margin to sodium boiling was calculated to be greater than 350 K (Ref. 3). Thus, the addition of the GEMs resulted in a major improvement in the PRISM response to a troublesome category of events, i.e., the ULOF sequences.

## 2.0 THE ALMR DESIGN

The ALMR plant, as presently proposed by G.E., consists of three identical power blocks of 465 MWe, for a total plant electrical rating of 1395 MWe (Table 2.1 and Figure 2.1). Each power block is comprised of three reactor modules with individual thermal ratings of 471 MWe. Each module has its own steam generator which is combined in each power block to feed a single turbine generator. The reactor module (Figure 2.2) is about 19 meters (62 feet) high and about 6 meters (20 feet) in diameter, and is placed in a silo (i.e., below grade).

Under normal operating conditions, four EM pumps draw sodium from the cold pool and drive it through eight pipes to the core inlet plenum. The sodium is heated as it passes upward through the fuel assemblies (hexagonal cans containing wire wrapped pins) and into the hot pool above the core region. The heat is transferred to the intermediate loop sodium by the Intermediate Heat Exchanger (IHX), as the primary sodium passes from the hot pool to the cold pool.

Table 2.1 ALMR Plant Design Data

|                                   |                             |
|-----------------------------------|-----------------------------|
| Reactors Modules Per Power Block: | Three                       |
| Number of Power Blocks:           | One/Two/Three               |
| Electrical Output:                | 465/930/1395 MWe            |
| Reactor Power:                    | 471 Mwt                     |
| Turbine Throttle Conditions:      | 7.58 MPa (Saturated)        |
| Primary Sodium                    | Inlet: 610K<br>Outlet: 758K |
| Secondary Sodium                  | Inlet: 555K<br>Outlet: 716K |
| Peak Fuel Pin Linear Power:       | 305 W/cm                    |
| Peak Fuel Burnup:                 | 135 MWd/kg                  |
| Refueling Interval:               | 18 months                   |

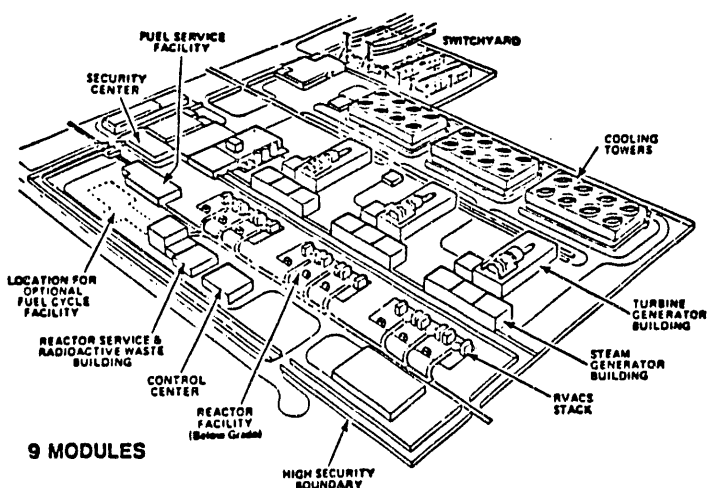


Figure 2.1 The 1395 MWe power plant with 3 power block

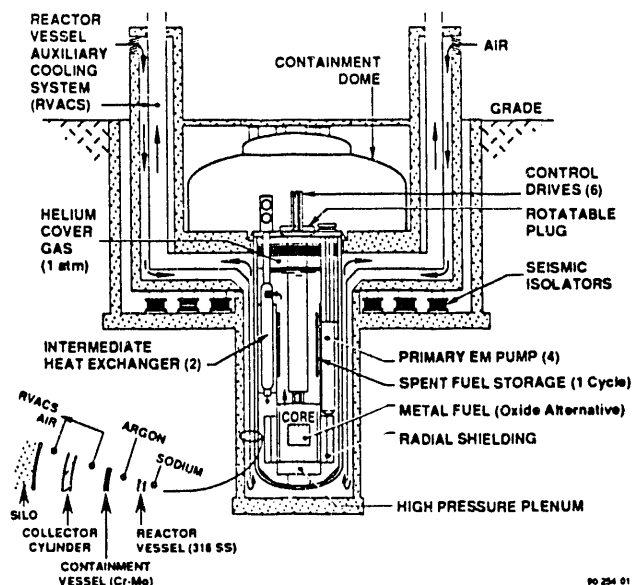


Figure 2.2 ALMR reactor module

The core design is illustrated in Figure 2.3. A "limited free bow" restraint system is utilized to assure an outward bow in the active core region of the assemblies as long as the peak temperatures are in the core center and decrease radially. The bowing is only one of several reactivity feedbacks that are essential to the design. The other significant feedbacks are Doppler, sodium density, fuel expansion, core radial expansion (via grid plate and above core load pads), the control rod drive line expansion, and the Gas Expansion Modules (GEMs). Most of these feedbacks are negative for off nominal conditions, since increasing the power and core average temperature causes the core criticality to decrease. This characteristic gives the core power the tendency to transition to a lower level at an elevated temperature (unless the sodium boils). Predictive calculations are performed to determine the rate, direction, and magnitude of the reactivity feedback components during postulated transients.

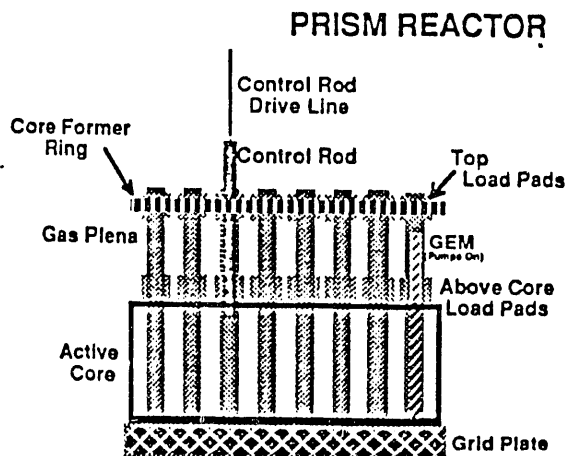


Figure 2.3 PRISM core

### 3.0 PRISM MODELING

The SSC (Ref. 4) and MINET (Ref. 5) codes were used in this analysis for complimentary purposes. SSC was developed at BNL for analyzing LMR transients. SSC can model core regions in detail, as well as the primary system, the IHX, intermediate loop, steam generator, and the major components of the ternary loop. However, alternate flow patterns that may develop during loss of heat sink events or certain loss of flow events can become very complicated, which requires the MINET flexibility for that part of the analysis.

#### 3.1 SSC Model

In Figure 3.1 a schematic drawing of the PRISM model is shown. The core was represented using 7 channels: fuel (or driver), internal blanket, radial blanket, control assembly, shield assemblies, hot driver, and hot internal blanket. Each channel includes 2 axial nodes in the lower shield, 6 axial nodes in the fuel region, and 4 nodes to represent the upper gas plenum.

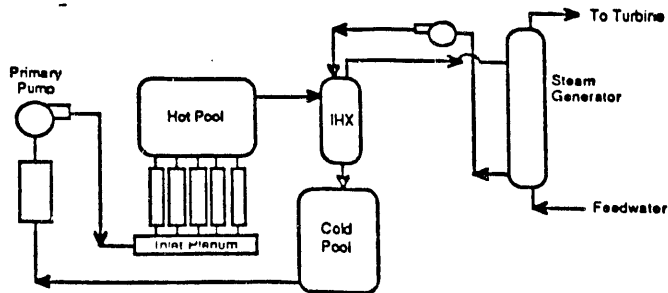


Figure 3.1 SSC representation of LMR systems

### 3.2 Reactivity Feedback Models

Several reactivity feedbacks are important in the passive shutdown response for the metal cores. Because of the smaller Doppler feedback in the metal core, reactivity feedbacks having little importance in oxide cores are significant in the metal core. The main reactivity feedbacks are discussed in the following sections.

#### 3.2.1 Doppler Feedback

As the fuel temperature increases, more neutrons are parasitically absorbed in the resonance energy range. For metal fuel, Doppler feedback is smaller than it is for oxide fuel because of the harder neutron energy spectrum, which places fewer neutrons in the resonance energy range. Also, due to high thermal conductivity, metal fuel operating temperatures are much lower than those in oxide fuel cores. This allows the power and temperature defects in a metal core to be small (~\$1.20), allowing the criticality and power level of the system to be more strongly influenced by other natural feedbacks.

#### 3.2.2 Axial Fuel Expansion

Metal fuel expands axially when it heats up. Axial expansion increases the core height and decreases the effective density of the core material. This increases the probability that a neutron will escape the core, giving a negative reactivity feedback.

All analyses performed using SSC assumed that the fuel is in contact with the HT9 clad. This is the most common state for the equilibrium core since only 25% of the core will be reloaded at each refueling, and the fuel is in an unlocked state, i.e., below 2 atom per-cent burnup, only briefly. Axial expansion is dominated by the clad after lockup since metal fuel is weak (i.e., small Young's Modulus). The fuel elongations in SSC calculations were calculated by using an average strain, weighted with Young's Modulus.

#### 3.2.3 Sodium Density Feedback

Thermal expansion of the sodium is the only significant positive reactivity feedback, except for the long term withdrawal of the control rod drive line with vessel heatup and a sodium void feedback. The thermal expansion results in fewer sodium atoms within and surrounding the core. The dominant effect is the reduction in collisions between neutrons and sodium atoms, which

hardens the neutron energy spectrum and yields a net positive reactivity feedback effect from the increased neutron importance.

The feedback formulation was set up to reference the sodium density at the refueling temperature. Each node was given equal weight within a given category (i.e., driver, internal blanket, and radial blanket).

### 3.2.4 Control Rod Drive Line and Vessel Thermal Expansion

The magnitude of this feedback is dependent upon the initial position of the control rods on the control rod worth curve. The control rod drive lines, which are in the upper internal structure and cantilevered from the top, expand when they are heated, inserting the control rods further into the fueled region, adding negative reactivity.

The thermal expansion of the reactor vessel ultimately limits the amount of negative reactivity inserted by the control rod drive line. The reactor vessel is also cantilevered from the top, and expands down and slowly withdraws the control rods from the core up to the control rod stop positions. The time constant for the reactor vessel is about 700s, while the control rod drive line expansion time constant is around 28s. Thus, the initial response to increased sodium outlet temperatures is a negative feedback, while the long term effect could end up being positive.

Control rod and vessel expansion are calculated in SSC using a single node to determine the temperature of the reactor vessel and control rod drive lines. The total elongated length is determined by subtracting the vessel expansion from the control rod drive line expansion to calculate the net control rod expansion into the core.

### 3.2.5 Radial Expansion

The radial dimension of the core is determined largely by assembly spacing. This spacing is determined by the grid plate below the core and by two sets of load pads above the core. When the structures heat up and expand it increases the core radius, which reduces the core average density in the radial direction. The effect increases neutron leakage and generates a negative feedback response.

SSC tracks the radial expansion of the core from thermal expansion only. This is achieved by tracking the structure temperatures at the above core load pads (just above the fueled area) and at the grid plate. In the SSC calculation, no credit was given for the thermal bowing of the assemblies. It is noted that the bowing effect may reduce the risk associated with several severe accident sequences. However, the total worth of the (limited-free) bowing carries significant uncertainties. Bowing should add negative reactivity to the system when core temperatures rise. At this time, it doesn't appear that bowing can insert any positive reactivity during any significant portions of the postulated accidents reviewed to date. Hence, neglecting it is generally a conservative assumption.

### 3.2.6 GEM Modeling

The GEM is essentially an empty assembly duct, sealed at the top, open at the bottom and connected to the high pressure in the inlet plenum of the core. The range of operation of the GEMs tested in FFTF can be seen in Figure 3.2. A hexagonal cross section duct, with a wall thickness slightly greater than the standard fuel and blanket duct, forms the unit. When the pumps are at full flow, the plenum pressure (minus the static heat to the GEM level) compresses the gas in the GEM cavity to the portion of the GEMs above the core. This causes more neutrons to be scattered and deflected back into the core, as compared to when

the gas is adjacent to the core. When the flow decreases, the trapped helium expands and drops the sodium level into the core region. As a result, fewer neutrons are scattered back into the core region. The effect increases as the gas expands into the fueled region core, until the gas-liquid interface drops below the core. At this point the maximum negative reactivity of 69 cents (i.e., 23 cents each) is inserted. This device offers a passive negative feedback which can help maintain an acceptable power-to-flow ratio during sudden loss of flow events.

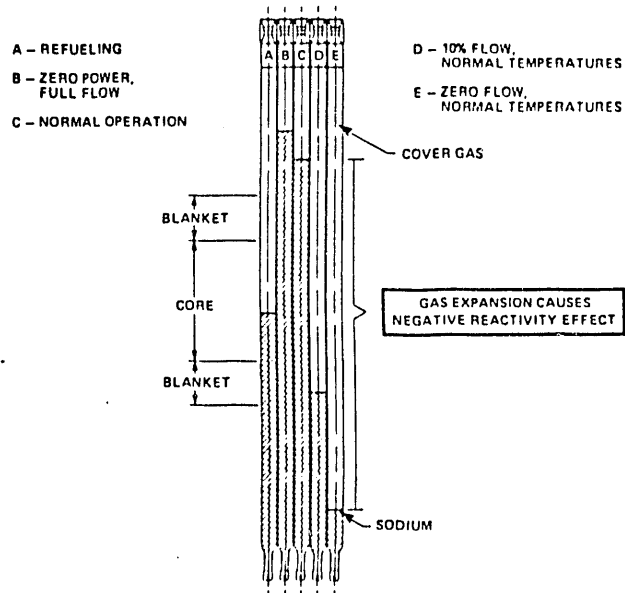


**Figure 3.2 Operation of the Gas Expansion Module (GEM) tested in FFTF (which has a similar behavior in PRISM)**

#### 4.0 RESULTS AND DISCUSSION

In this section, the PRISM system response is evaluated for an ULOF event where one EM pump loses its coastdown following a pump trip without a SCRAM. The SSC code was used to predict the behavior of the original (1987) and the revised (1989) PRISM design. There are several differences between the two versions of PRISM, but most of them are not significant to this discussion, except for the addition of the GEM module.

##### 4.1 The Scenario

Since an EM pump has virtually no inertia, it was necessary for GE to use synchronous machines to provide artificial coastdowns to the EM pumps when they are tripped. These machines, which are little more than flywheels coupled with motor generator units, are operated continuously so that if there is a power loss, or other malfunction, then there will be a resultant coastdown. As the synchronous machine is coasting down, the rotational energy is tapped and diverted to the EM pumps, which experience a gradual, pre-programmed reduction in power.

The Unscrammed Loss of Flow (ULOF) event, with three out of the four EM pumps coasting down, begins at nominal operating conditions. For whatever reason, a signal is sent to trip the pumps and SCRAM the reactor. The control rods are assumed not to SCRAM, but the pumps trip. At the instant the pumps switch from A/C to the synchronous machine power, one out of the four EM pumps is assumed to fail. An EM pump is essentially a pipe with coils surrounding it to generate the magnetic field necessary to force the sodium through the device. Once the EM pump fails, the pump acts like a pipe. The high pressure at the core inlet plenum causes sodium to back up through the failed pump into the cold pool. Thus, the sodium being delivered to the inlet plenum by the three remaining EM pumps is spilt. Some passes through the core while the rest returns through the failed pump into the cold pool. Without a corresponding drop in power, the power-to-flow ratio will quickly increase and reduce the safety margins.

The analysis of this event was complicated by the need to predict the flow spilt between the flow going back through the failed pump and the flow that proceeds through the core. The sodium flow bifurcation was predicted by the MINET code, while the resulting power was predicted by the SSC code. Since the reactor power level and sodium flow rate are closely coupled, a few passes between MINET and SSC were needed to determine the appropriate sodium flow rate passing through the PRISM core during this event.

In the MINET model, the pumps were represented individually, using a fairly detailed pump head and the torque curves provided by GE. Complexity is caused by the failure of one pump, which creates an open pathway for the sodium to short-circuit back to the inlet of the other pumps from the core inlet plenum through the failed pump. Normally, the flow through each pump drops in half, and then begins the coastdown process; but when one pump fails, the flow drops to about 17% and then starts the coastdown. The coastdown is more protracted for this case. The difference in behavior is caused by the open line (i.e. the failed pump), which greatly reduces the flow resistance in the flow circuit and reduces the torque on the flywheel, which increases the time for the pumps to coastdown. Once the flow coastdown was determined, it was programmed in SSC to drive the transient calculations.

#### 4.2 Three Pump Coastdown Without GEMs

SSC predictions of a 3 pump coastdown, after a pump trip, without a SCRAM, are shown in Figures 4.1 through 4.4. The EM pump failure causes the core flow to drop quickly (Figure 4.1). The power is predicted to lag the core flow by about 12s. This results in a power-to-flow increase during that period. In Figure 4.2, the peak temperature at the fuel centerline was predicted to reach 1385K, which is about 119K above the fuel's solidus temperature; thus, the fuel centerline is predicted to be in a melted phase. The peak sodium temperature in Figure 4.3 indicates that the sodium reaches the saturation point. SSC did predict the presence of some sodium boiling at the core exit.

The components of the reactivity feedbacks generated from the "passive shutdown" system in PRISM is shown in Figure 4.4. The total reactivity initially increases to be slightly positive for the first few seconds, but changes over to being a negative value by 3.0s. The total reactivity continues to decrease, and by 20s, it reaches -38¢. Negative reactivity is generated because the reduction in core flow results in a sodium temperature increase from the core power-to-flow mis-match. The negative feedback from axial expansion and Doppler feedback counteracts the sodium density effect. After about 3s, the radial expansion begins to contribute, and between the three, they counteract the positive sodium density effect and produce a net negative reactivity feedback. Therefore, Figure 4.4 demonstrates the "passive shutdown system" is activated by the thermal expansion of core components that are affected by the increase in temperature within the core. However, during a situation when the flow drops quickly, there exists a period of time where the (positive) density feedback

could outpace the negative feedbacks and cause a power excursion, or delay in the transition to a lower power level.

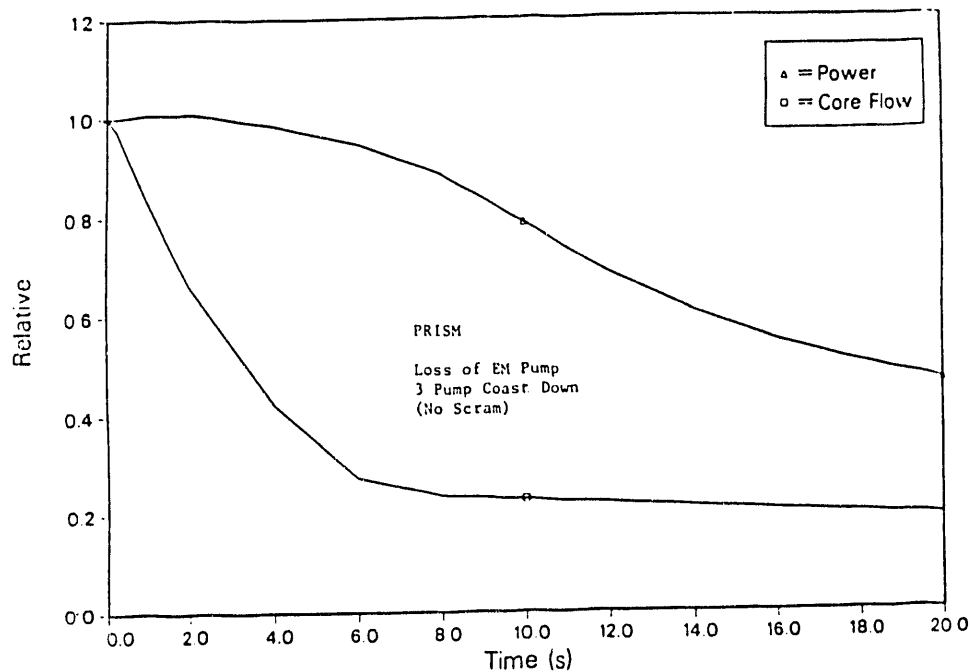


**Figure 4.1** SSC prediction for PRISM 3 pump coastdown:  
relative power and core flow

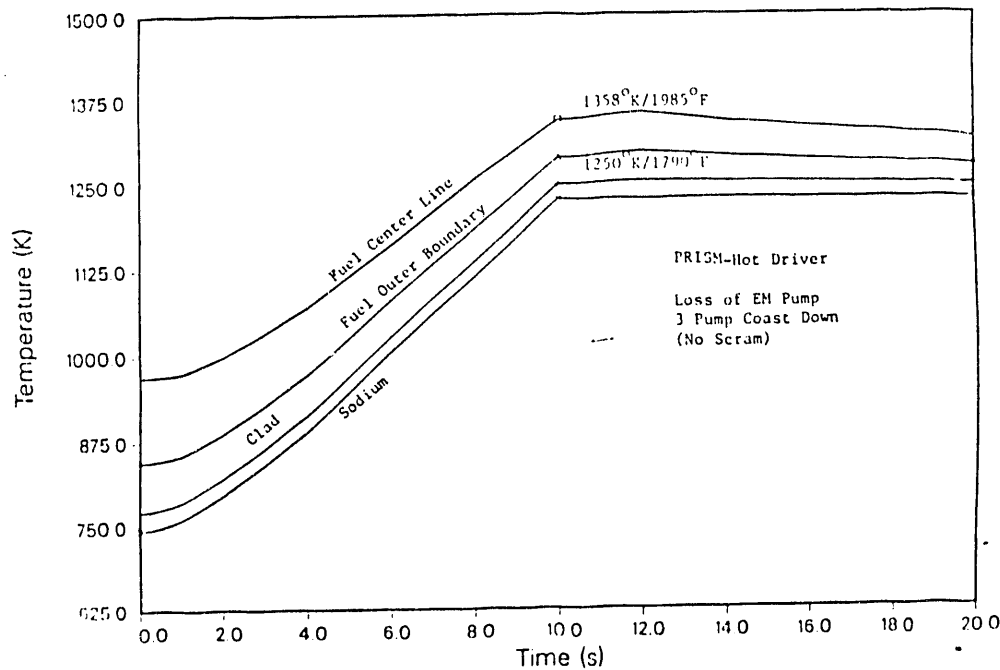


**Figure 4.2** SSC prediction for PRISM 3 pump coastdown:  
peak temperatures

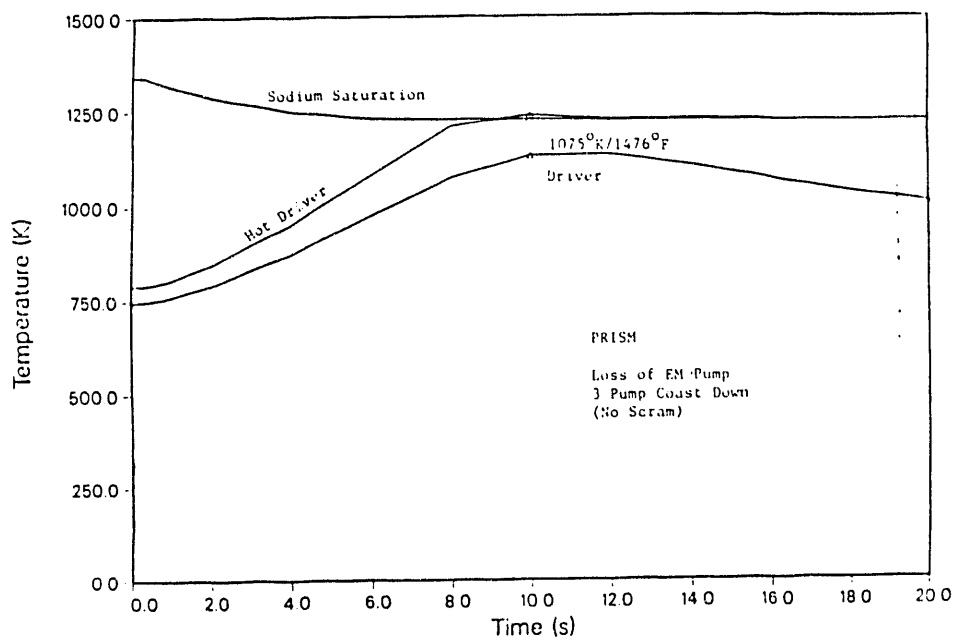


**Figure 4.3 SSC prediction for PRISM 3 pump coastdown: outlet and saturation temperatures**

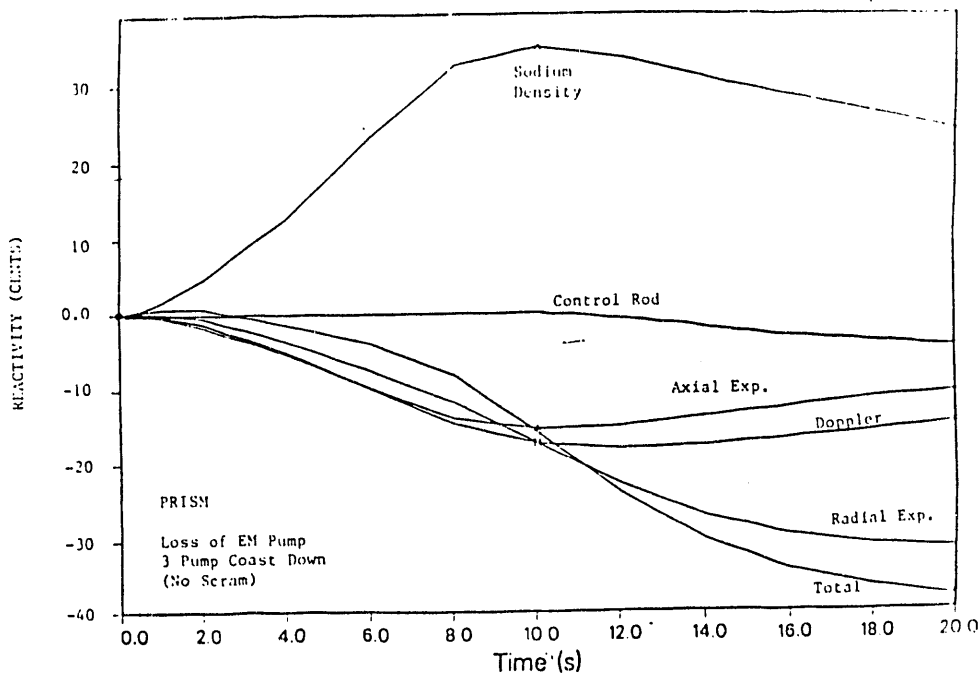


**Figure 4.4 SSC prediction for PRISM 3 pump coastdown: reactivity feedbacks**

#### 4.3 Three Pump Coastdown With GEMs

The same scenario was used for this calculation, but the SSC model had the three GEMs included. The core flow is shown in Figure 4.5 to drop quickly and the power drops along with it. This behavior preserves an acceptable power-to-flow ratio during this phase of the event. By 600s, the power generated in the core was from decay heat only. In Figure 4.6, the fuel, clad, and sodium temperature for the hottest location in the core shows only a small increase from steady state and the temperatures level off at about 1000K. This is not a high enough temperature to challenge the fuel integrity, or to damage the clad. The margin to sodium boiling was significantly increased by the addition of the GEMs, as can be seen in Figure 4.7 (and compared against Figure 4.3).

The decrease in power with the core flow can be understood by reviewing the reactivity feedbacks shown in Figures 4.8 through 4.10. The total reactivity, which is the summation of radial, axial and control rod drive line expansion and the effects from Doppler, sodium density, and the GEMs, can be seen in Figure 4.8 to drop to a -50 cents immediately, and to -\\$1.1 by 1000s. The radial expansion (which is composed of the Above Core Load Pad (ACLP) and core grid plate in Figure 4.8.) and sodium density term counterbalance each other, as shown in Figure 4.9 while the axial expansion terms go positive, indicating the fuel has contracted because it actually cooled down in comparison to the steady state condition. After 600s, the reactor vessel went into a well established natural circulation condition and the feedbacks approached a new quasi-static condition.

As shown in Figure 4.10, the Doppler initially adds positive reactivity because the fuel cools down relative to the steady state conditions. The increase in temperature in the upper plenum caused the control rod drive line to expand enough to generate -25 cents of reactivity by the end of the event. The remaining term in this plot is the GEM reactivity. It can be seen that as the pressure dropped in the core inlet plenum, the gas bubble expanded into the core region and caused an increase in neutron leakage and generated a fast -40 cents of reactivity. Figure 4.11 shows the GEM level as a function of time. By about 575s, the GEMs inserted the full -69 cents of negative reactivity.

This calculation demonstrates that the GEMs have a major impact on the safety margins. As the result of adding three GEMs to PRISM, the seizure of 1 pump during a coastdown, without a SCRAM, has gone from a very severe challenge to the fuel and sodium boiling conditions, to an event that PRISM can survive without damage.

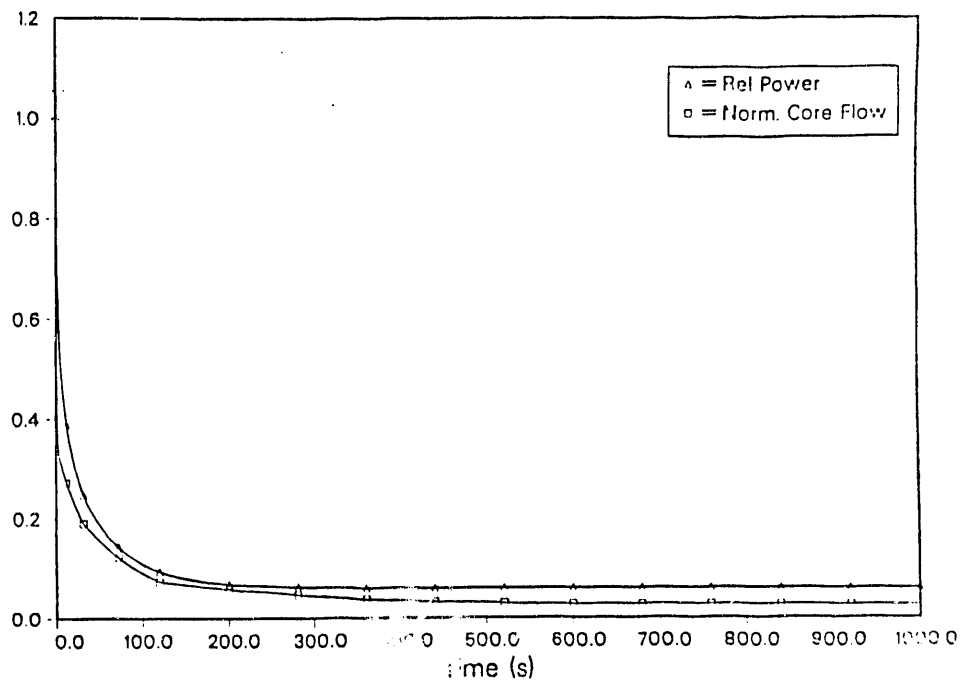


**Figure 4.5** Predicted relative power and normalized core flow from SSC for a ULOF with 1 pump seized

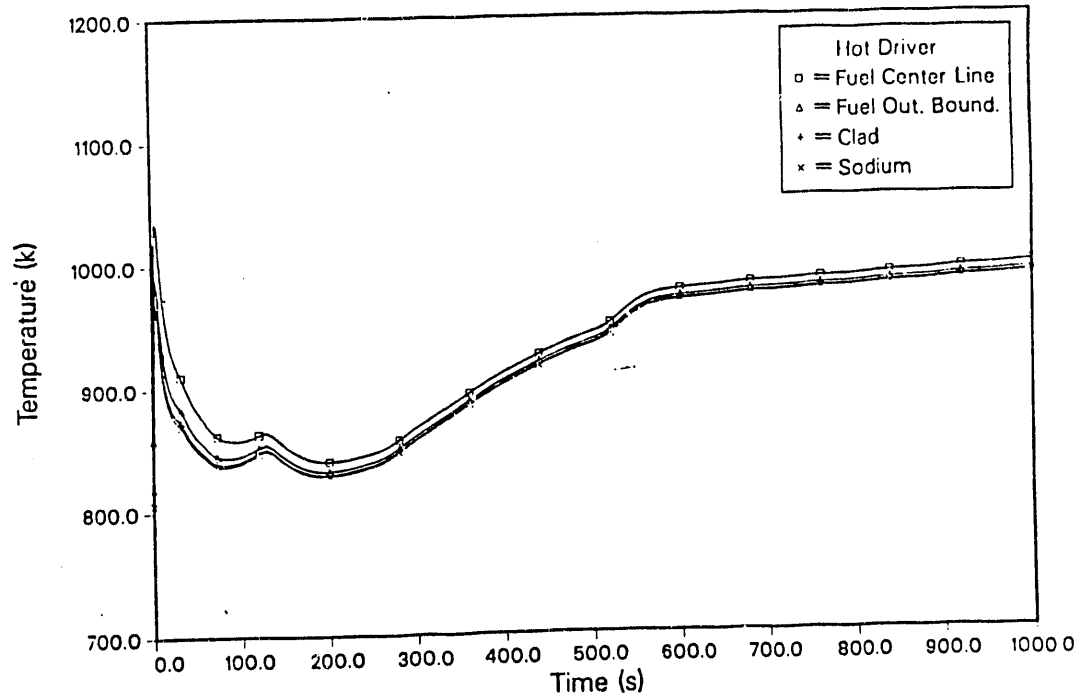


**Figure 4.6** Predicted fuel temperature distribution for the top node (i.e., 1,346 m-1.122m) of a fuel pin from SSC for a ULOF with 1 seized pump

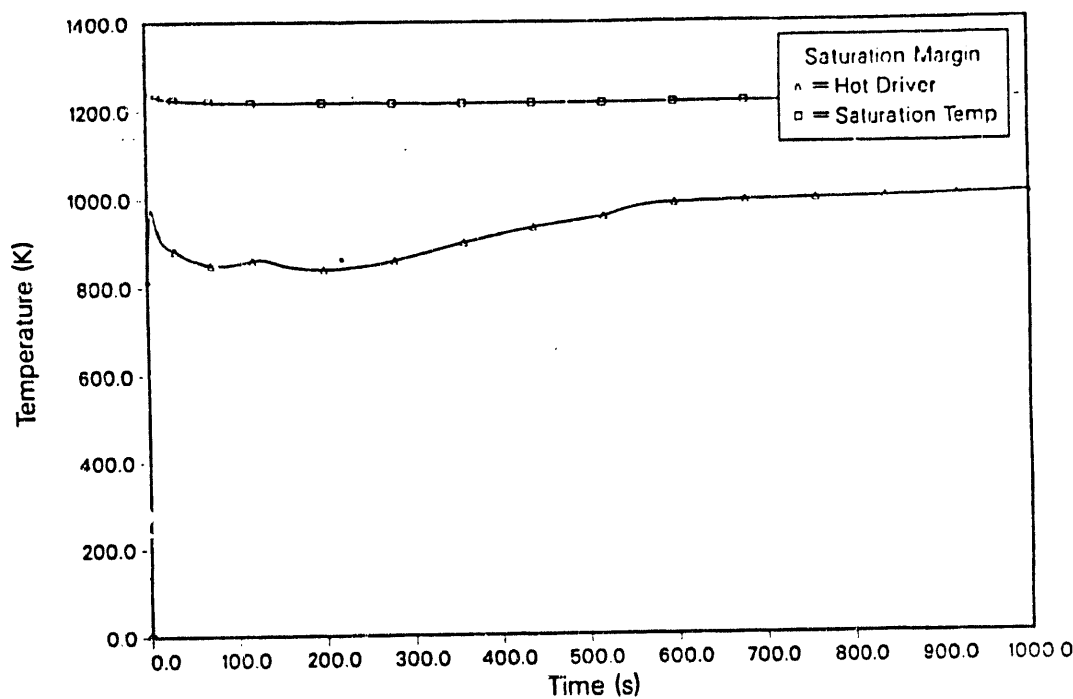


**Figure 4.7** Predicted margin to sodium saturation from SSC for a ULOF with 2 pumps seized

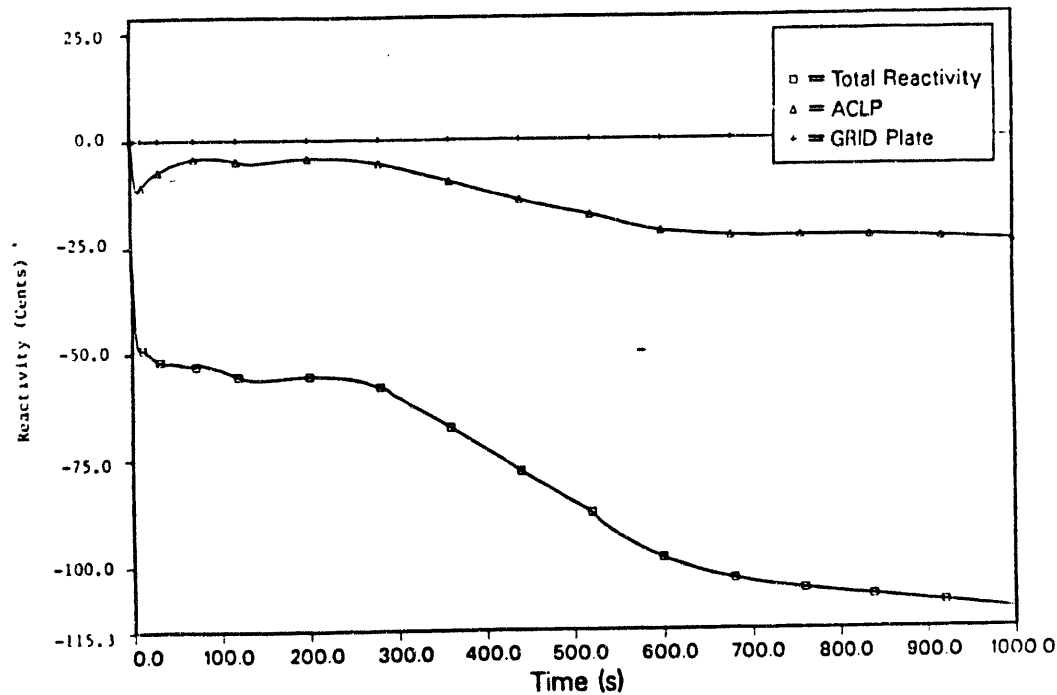


**Figure 4.8** Predicted total ACLP, and grid plate reactivity feedback from SSC or a ULOF with 1 pump seized

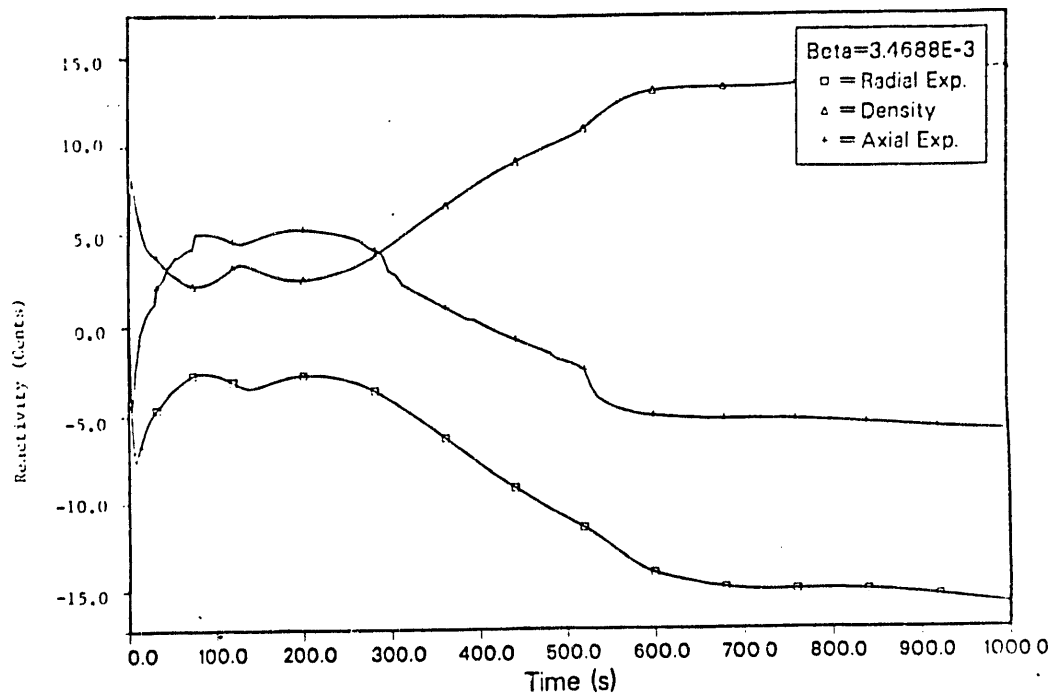


**Figure 4.9** Predicted core radial expansion, sodium density, and axial expansion reactivity feedback from SSC for a ULOF with 1 pump seized

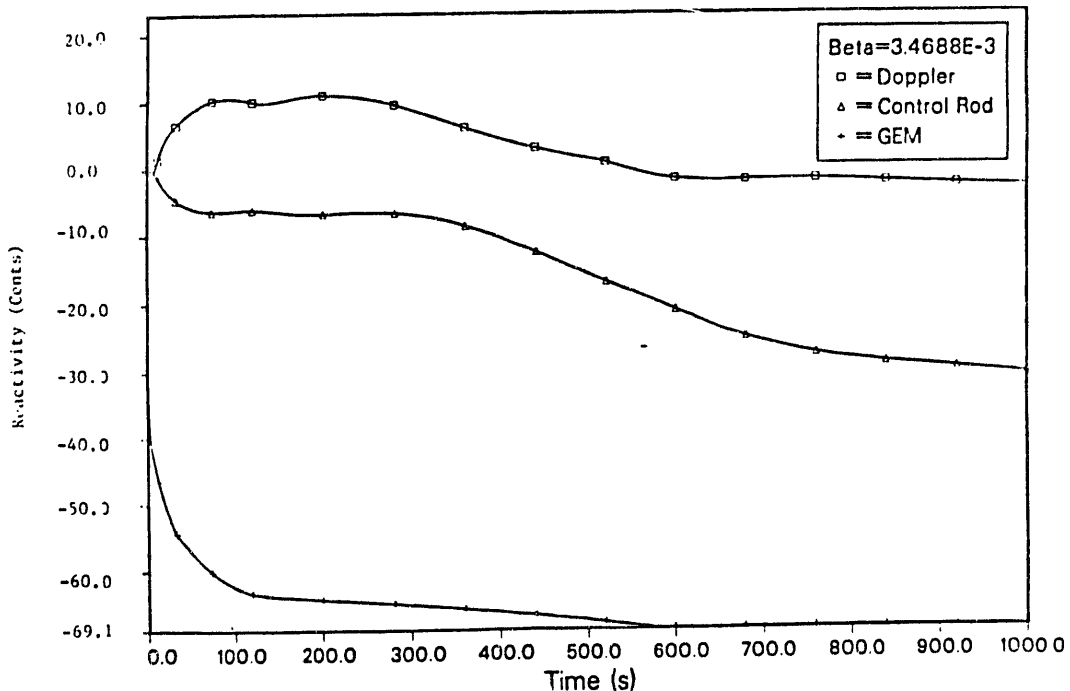


**Figure 4.10** Predicted Doppler, control rod drive line thermal expansion and GEM reactivity feedback from SSC for a ULOF with 1 seized pump

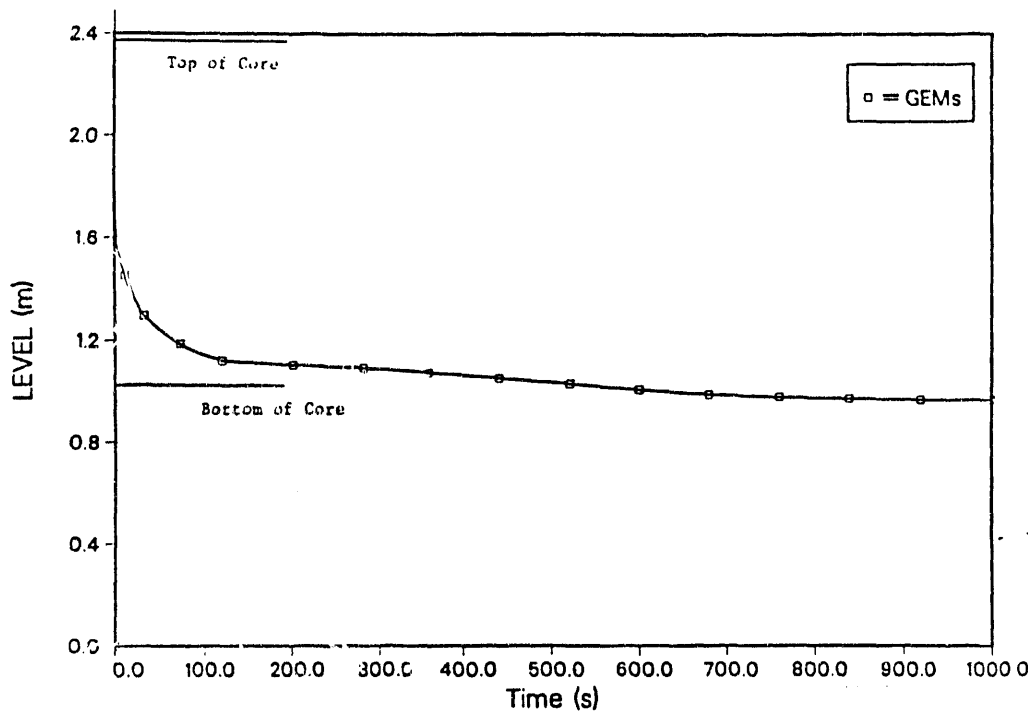


Figure 4.11 Predicted sodium level in GEMs from SSC for a ULOF with 1 pump seized

## 5.0 SUMMARY

The inclusion of the PRISM GEMs in the SSC model resulted in very different behavior during postulated ULOF events, when compared to the previous design. The initial design had only the passive shutdown mechanisms to preserve an acceptable power-to-flow ratio. This sometimes resulted in a fast increase in the power-to-flow ratio, which caused the margin to sodium boiling to be only a few degrees. Thus, in the original PRISM design, ULOF events that postulated missing one or more EM pump coastdowns, as provided by the "synchronous machines" (motor-generator sets running in parallel), had little or no safety margin. Fuel temperatures in the hot and average channel were calculated to be 1358K (which is above the solidus temperature of metal fuel) and 1147K (Ref. 2). However, after the GEMs were added, the loss of one EM pump coastdown became a benign event. The GEM worth dominated the other reactivity feedbacks and, essentially, the GEMs responded like passive control rods. The fuel temperatures quickly dropped below operating temperatures, while the margin to sodium boiling was calculated to be greater than 350 K (Ref. 3). Thus, addition of the GEMs resulted in a major improvement in the PRISM response to a troublesome category of events, i.e., the ULOF sequences.

## 6.0 REFERENCES

1. R.R. Landry, T.L. King, and J.N. Wilson, "Draft Pre-application Safety Evaluated Report for Power Reactor Inherently Safe Module Liquid Metal Reactor", Nuclear Regulatory Commission Report, NUREG-1368, September 1989.
2. G.J. Van Tuyle, G.C. Slovik, B.C. Chan, R.J. Kennett, H.S. Cheng, and P.G. Kroeger, "Summary of Advanced LMR Evaluations - PRISM and SAFR", Brookhaven National Laboratory Report, NUREG/CR-5364, BNL-NUREG-52197, October 1989.
3. G.J. Van Tuyle, G.C. Slovik, B.C. Chan, A.L. Aronson, and R.J. Kennett, "Evaluations of 1990 PRISM Design Revisions", Brookhaven National Laboratory Report, NUREG/CR-5815, BNL-NUREG-52311, March 1992.
4. J.G. Guppy, et al., "Super System Code (SSC, Rev. 0) An Advanced Thermohydraulic Simulation Code for Transients in LMRBRs", NUREG/CR-3169, BNL-NUREG-51659, April 1983.
5. G.J. Van Tuyle, T.C. Nepsee, and J.G. Guppy, "MINET Code Documentation", NUREG/CR-3668, BNL-NUREG-51742, Brookhaven National Laboratory, February 1984.

## DISCLAIMER

This report was prepared as an account of work sponsored by an agency of the United States Government. Neither the United States Government nor any agency thereof, nor any of their employees, makes any warranty, express or implied, or assumes any legal liability or responsibility for the accuracy, completeness, or usefulness of any information, apparatus, product, or process disclosed, or represents that its use would not infringe privately owned rights. Reference herein to any specific commercial product, process, or service by trade name, trademark, manufacturer, or otherwise does not necessarily constitute or imply its endorsement, recommendation, or favoring by the United States Government or any agency thereof. The views and opinions of authors expressed herein do not necessarily state or reflect those of the United States Government or any agency thereof.

END

DATE  
FILMED

5/20/93

